Appl. Phys. B 79, 1021–1025 (2004)
DOI: 10.1007/s00340-004-1663-7

Applied Physics B
Lasers and Optics

M.G. SCHÄTZEL[1,✉]
F. LINDNER[1]
G.G. PAULUS[1,2,3]
H. WALTHER[1,2]
E. GOULIELMAKIS[4]
A. BALTUŠKA[4]
M. LEZIUS[4,5]
F. KRAUSZ[1,2,4]

Long-term stabilization of the carrier-envelope phase of few-cycle laser pulses

[1] Max-Planck-Institut für Quantenoptik, Hans-Kopfermann-Str. 1, 85748 Garching, Germany
[2] Ludwig-Maximilians-Universität München, Am Coulombwall 1, 85748 Garching, Germany
[3] Department of Physics, Texas A&M University, College Station, TX 77843-4242, USA
[4] Institut für Photonik, Technische Universität Wien, Gusshausstr. 27, 1040 Wien, Austria
[5] Institut für Ionenphysik, Universität Innsbruck, Technikerstr. 25, 6020 Innsbruck, Austria

Received: 22 June 2004/Revised version: 14 September 2004
Published online: 26 October 2004 • **© Springer-Verlag 2004**

ABSTRACT The temporal variation of the electromagnetic field of a few-cycle laser pulse depends on whether the maximum of the pulse amplitude coincides with that of the wave cycle or not, i.e., it depends on the phase of the field with respect to the pulse envelope. Fixation of this 'carrier-envelope' phase has only very recently become possible for amplified laser pulses. This paved the way for a completely new class of experiments and for coherent control down to the attosecond time scale because it is the field and not the pulse envelope which governs laser-matter interactions. However, this novel technique still affords much potential for optimization. In this paper we demonstrate a novel stabilization scheme for the carrier-envelope phase that not only guarantees a stable phase for arbitrarily long measurements, but also makes it possible to restore any given phase for an application after a pause of any kind. This is achieved by combining a stereo-ATI phase meter with a feedback loop to correct phase drifts inside and outside the laser system.

PACS 07.05.Dz; 32.80.Rm; 42.50.Hz

1 Introduction

Femtosecond laser technology has greatly promoted fundamental investigations of strong-field physics. An essential achievement was the realization of extremely short laser pulses comprising only few optical cycles at near-infrared wavelengths [1, 2]. To a good approximation, the electric field $\mathcal{E}(t)$ of such a short laser pulse can be described as $\mathcal{E}(t) = \mathcal{E}_0(t)\cos(\omega_L t + \phi)$. Besides the carrier frequency ω_L and pulse envelope $\mathcal{E}_0(t)$, the phase difference ϕ between the pulse envelope and its carrier wave, conventionally termed carrier-envelope (C-E) or "absolute" phase, also plays a decisive role in the temporal evolution of the electric field. Although this has been known for years (see, for example, [3]), the first C-E phase effect was only recently detected, with the C-E phase randomly fluctuating [4].

While phase stabilization of femtosecond oscillators can now be routinely achieved [5–8], a phase-stabilized laser system with a power amplifier was only recently realized [9]. Using amplified phase-stable few-cycle laser pulses, phase effects were measured in high-order harmonic generation (HHG) [9], above threshold ionization (ATI) [10], and non-sequential double ionization (NSDI) [11]. A growing number of publications also examines these effects theoretically [12–19]. Phase stabilization of the amplified laser system works very well on moderate time scales, but certain experiments need phase stability over an extended period of several hours, which so far cannot be guaranteed. A new stabilization scheme for this purpose is demonstrated here.

✉ Fax: +49-89-32905-200, E-mail: Michael.Schaetzel@mpq.mpg.de

2 Principles

The basic idea for stabilizing the carrier-envelope phase of a laser system is to use the f-to-$2f$ technique [5, 6]. It allows the carrier-envelope offset frequency f_{CEO} to be directly measured and conveniently stabilized in a servo loop. This servo loop either controls an acousto-optic modulator (AOM) to modify the pump power of the laser oscillator [20] or controls a piezo to swivel a mirror inside the cavity [21]. Both methods change the relative value of v_{group} and v_{phase}, thereby shifting f_{CEO}. A phase-stable offset frequency f_{CEO} is equivalent to a stable (and known) drift of the C-E phase ϕ; for $n = f_{rep}/f_{CEO}$ every nth pulse has an identical phase.

To generate stabilized high-power pulses, n is chosen as an integer and the ratio of the repetition rates of the oscillator and multipass amplifier is tuned so that only pulses of identical ϕ are amplified. The residual C-E phase drift after amplification is monitored by a second f-to-$2f$ interferometer and compensated in the same electronic loop controlling the oscillator [9]. Few-cycle pulses are then generated by spectral broadening of the amplified pulses in a hollow fiber [1] filled with neon and subsequent compression by reflections off chirped multilayer dielectric mirrors [22].

While this approach is very reliable in locking the phase ϕ, its value is not known and it is extremely sensitive to experimental parameters. Consequently, if the phase lock is lost it is not possible to lock to the same value as before, since the system has to be realigned. In addition, long-term stability cannot be guaranteed over extended periods of time (see Fig. 1), even if relocking does not become necessary. The reason for this is small phase drifts which are not always compensated by the f-to-$2f$ technique. Two particularly noteworthy imperfections in the stabilization scheme are responsible for this: First, the f-to-$2f$ stabilization scheme relies on comparison

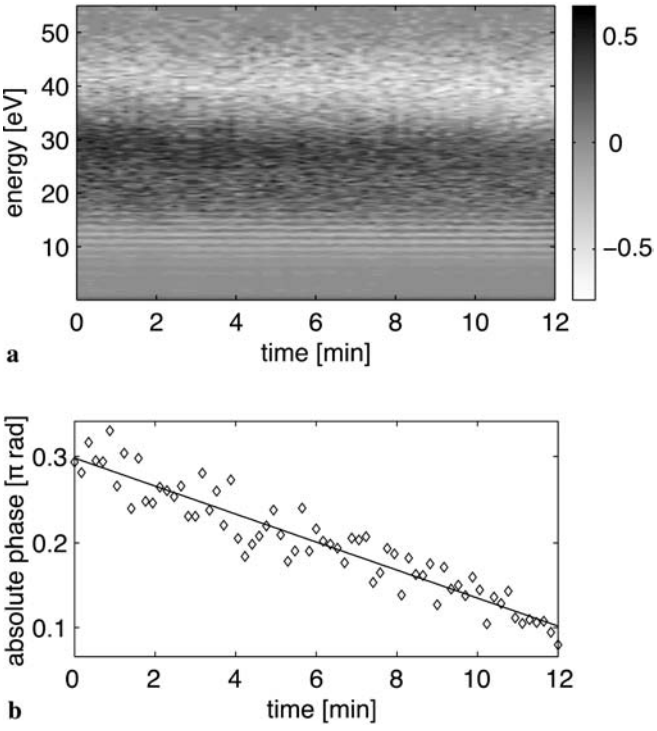

FIGURE 1 (**a**) Measured left/right asymmetry $[(L-R)/(L+R)$, where L (R) denotes the number of electrons seen on the left (right) detector] of the electron spectra in the stereo-ATI experiment, as a function of electron energy and time. *Dark colors* represent dominant left emission, *bright colors* dominant right emission. (**b**) Respective phase retrieved from panel (**a**) and the underlying raw data utilizing the energy range of 20–40 eV. Due to limited theoretical understanding the absolute value of the phase has an uncertainty of $\pi/10$, but the relative phase values are far more precise. Each experimental point corresponds to an integration time of 10 s or 10^4 laser shots. Note that the visible phase jitter is mainly due to the short integration time chosen (corresponding to a count rate of roughly 2200 electrons per detector in the stated energy window) and can be justified by purely statistical means. It does not represent the shot-to-shot phase jitter of the laser. A clear linear phase drift (*solid line*) of ~ 50 mrad/min can be detected, which represents a typical value. The actual stability of the laser system varies with time, as does the value of the phase drift

of frequencies in the red and blue wings of the spectrum. Since dispersion at these wavelengths is different from the center wavelength decisive for the carrier-envelope phase, the present stabilization will introduce small phase errors as soon as it starts to compensate any drifts in the amplifier [23]. Second, the feedback for the phase stabilization is taken after the femtosecond laser amplifier but before the pulses are spectrally broadened in the hollow fiber and recompressed to few-cycle pulses. Any drifts in the latter part, possibly originating from beam-pointing instabilities and amplitude-phase coupling, are therefore not compensated. The first problem mentioned depicts an inherent shortcoming of the f-to-$2f$ scheme, namely the inability to correctly detect phase drifts induced outside the cavity of the mode-locked oscillator, while the second one merely is a technical problem.

Combining the stereo-ATI phase meter with an external stabilization loop as presented in this paper offers a powerful solution to these problems. The experimental setup is described in Sect. 3. The underlying physics of the stereo-ATI experiment has already been described elsewhere [4, 10] and is only briefly reviewed.

Above-threshold ionization is a prominent effect in photoionization at high intensity [24]. More photons than necessary for ionization can be absorbed and, accordingly, photoelectrons with a kinetic energy of many times the photon energy can then be observed. In the strong-field limit [25], a simple semi-classical model (for a review see [26]) explains this as follows: At some time t_0, an electron enters the continuum due to tunnel ionization. The laser's electric field then accelerates the electron away from the atom. When the field changes direction, it may drive the electron back to its parent ion, where it may scatter either elastically or inelastically. The electron is then further accelerated by the electric field. In the electron spectra, the rescattering mechanism creates a plateau-shaped annex at the high-energy (> 25 eV) side of the nearly exponentially decreasing low-energy 'direct' electrons that did not undergo rescattering [27]. A simple classical calculation yields a maximum kinetic energy of $2\,U_\mathrm{p}$ for direct electrons and $10\,U_\mathrm{p}$ for elastically 'rescattered' electrons (the so-called 'cut-off'). U_p denotes the ponderomotive energy $U_\mathrm{p} = \mathcal{E}^2/4\omega_\mathrm{L}^2$ (atomic units). Quantum mechanics considerably softens these sharp energy limits.

Due to the nonlinear nature of ATI, the carrier-envelope phase of the laser pulse is expected to play an important role [15, 18]. Not only does the position of the cut-off depend on the phase ϕ, but also the number of cycles contributing to a given energy, leading to phase-dependent peak structures. The idea of phase detection is to exploit this anisotropic electron emission. With linearly and circularly polarized light a significant left-right asymmetry is expected.

3 Experimental setup

The experimental setup consists of two parts: (i) the stereo-ATI phase meter (Fig. 2) combined with an appropriate software algorithm to determine the carrier-envelope phase ϕ of the laser pulses and (ii) a feedback loop controlling a device to keep (or set) ϕ at a given value. To use the combined machinery of laser and stabilization for an independent experiment applying phase-stable few-cycle pulses, the beam has to be split as shown in Fig. 3.

For all measurements in this publication (Figs. 1, 4, 5, 6 and Sect. 4) the same phase-stabilized laser system was used. It generates nearly transform-limited few-cycle pulses of 5.4 fs FWHM with an energy of up to 400 μJ per pulse at a central wavelength of 760 nm. The repetition rate is 1 kHz. A detailed description of the laser can be found in [9] and especially in section VI of [28]. The phase stabilization scheme described here, however, can be used with any amplified phase-stable laser system, given it provides sufficiently short pulses.

The aquisition of the photo-electron spectra relies on time-of-flight spectroscopy. Two opposing electrically and magnetically shielded drift tubes 50 cm in length are mounted in an ultrahigh-vacuum ($p < 10^{-7}$ mbar) apparatus. Rare-gas atoms fed in through a nozzle from the top are ionized by the few-cycle laser beam, which is focused with a concave mirror of focal length 250 mm (f-number 30). The laser polarization is linear and parallel to the flight tubes. Slits with a width of 250 μm are used to discriminate electrons created outside the laser focal region chosen. Electrons emitted to the left and

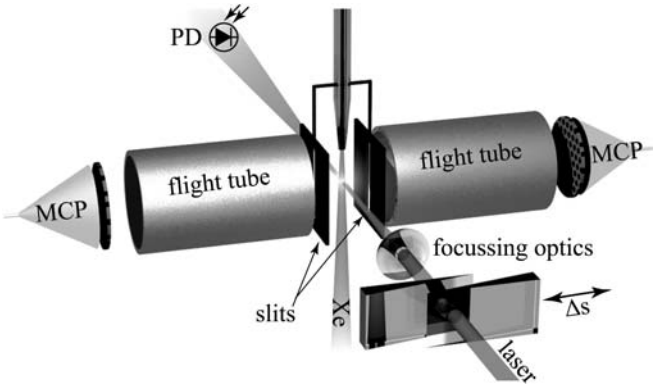

FIGURE 2 "Stereo-ATI" spectrometer. PD: photodiode, MCP: microchannel plate. A pair of glass wedges (apex angle 2.8°) is used to adjust the carrier-envelope phase. The lens shown in the sketch is in reality a concave mirror. For more details see text of Sect. 3

to the right are independently detected by two 18-mm diameter microchannel plates (MCP, Burle BiPolar TOF Detector). The time-of-flight is measured by two computer-hosted multiscalers (FAST 7886, FAST ComTec, Oberhaching, Germany) with a time resolution of 0.5 ns. The start signal is generated by a fast photodiode (PD), recording the arrival of the laser pulse; the stop signal by the MCPs, recording the arrival of each electron at the end of the drift tube. The electrons' time-of-flight is then used to calculate their kinetic energy. For each laser shot about 50 electrons are recorded at each MCP. The characteristic appearance of the apparatus eventually resulted in the term stereo-ATI spectrometer.

The gas used for these experiments is xenon, known to exhibit a strong ATI plateau for few-cycle laser pulses [29]. Absorption of eight photons is necessary in order to subdue the ionization threshold, but processes of much higher order can be observed. The pulse energy is attenuated to 20 μJ. The pair of slits can be moved along the beam propagation direction from outside the vacuum apparatus. This allows the desired intensity to be selected, in our case $\approx 8 \times 10^{13}$ W cm^2.

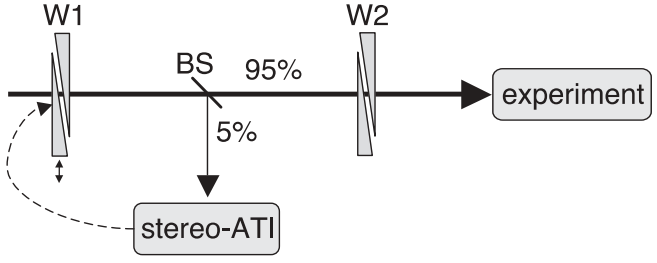

FIGURE 3 Experimental arrangement used in order to run an independent experiment while guaranteeing a stable carrier-envelope phase for an extended length of time. The laser is divided with a beam splitter (BS) to steer a small part of the beam to the stereo-ATI setup. Less than 5% of the pulse energy (≈ 20 μJ for a pulse of 5 fs FWHM) is sufficient for ATI, leaving essentially the full power available. Careful dispersion compensation is achieved by separately tuning the amount of glass in the beam paths, ensuring short pulse durations in both the stereo-ATI and the other experiment of interest. W1 is the glass wedge controlled by the feedback loop to keep ϕ constant in the whole beam path afterwards. W2 can be used to conveniently change ϕ in the experiment without affecting any other parameter. Basically, everything up to W2 can be viewed as part of an ultra-stable laser system for any user not interested in the origin of the laser pulses needed to perform the experiment

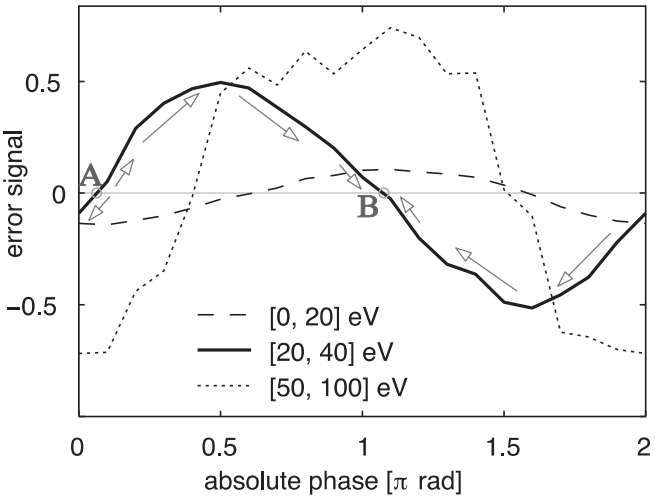

FIGURE 4 Measured error signal as a function of the carrier-envelope phase for three different energy windows. The integration time is fixed to 40 s for each experimental point. The signal is calculated from the measured spectra as $(L-R)/(L+R)$, considering only the given energy window. The phase stabilization idea is as follows, denoted by the *gray arrows*: A proportional amount of glass is added (removed) for positive (negative) error signals. Thus, position A is unstable, whereas position B is stable

Considerably higher intensities would result in detrimental saturation effects and, in particular, would smear out the characteristic plateau structure, which shows the most dramatic phase effects.

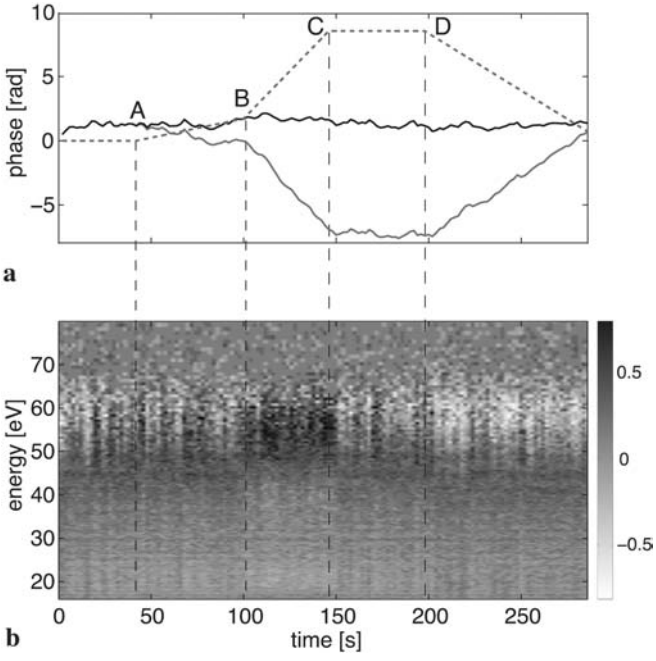

FIGURE 5 (**a**) Phase variation deliberately introduced by a pair of glass wedges (*dotted line*) as a function of time. The pair of wedges driven by the stereo-ATI servo-loop (*lower gray line*) compensates in real time the induced phase drift, leading to a resulting total glass thickness (*black line*, converted to phase values) approximately constant. The induced phase drift was +1.8 rad/min (A–B), +9.0 rad/min (B–C), 0 rad/min (C–D), −5.4 rad/min (D–end). (**b**) Measured left/right asymmetry (same color coding as in Fig. 1) as a function of electron energy and time. From this the necessary movement of the 'corrective' wedge was derived

Careful analysis of the acquired ATI spectra yields the absolute value of the phase ϕ in the interaction region to within an accuracy of $\pi/10$ rad [10]. The acquisition of two ATI spectra in opposite directions immediately gives the value of the phase, without requiring comparison with other spectra corresponding to different phases. So far the characterization is not fully automated, since the photo-electron spectra depend not only on the phase but also on the atom species [29] and the intensity (dependent on both pulse length and power) in the interaction zone. However, for stabilization the actual value of ϕ need not be known and the sensitivity to phase deviations is much higher than the accuracy stated.

An immediate way of generating a phase-dependent error signal is to examine the measured spectra for asymmetries in the emission to the left and right. As shown in Fig. 4, the contrast of this method strongly depends on the energy region of the electrons considered. This is not surprising, since high-energy electrons are much more affected by the shape of the electric field due to the time delay introduced by the rescattering mechanism. The disadvantage of high-energy electrons is their considerably lower abundance as compared with low-energy electrons, which show a comparatively weak phase dependence. For an optimum choice of electrons both contrast and count rate have to be considered. A good compromise is obtained by considering the plateau range (here typically 20–40 eV). A proper integration time to acquire the error signal is also very important. Short integration times produce significant phase noise, whereas long integration times result in slow feedback, thus limiting the servo bandwidth. Since the stereo-ATI apparatus is supposed to correct long-term phase drifts, relatively long integration times can be used. Note that, regardless of the energy range and integration times chosen, better results are expected for shorter laser pulses, due to the stronger phase effects.

After detection of a phase drift, a means of correcting it is needed. Besides the standard methods of pump-power modulation or swivelling of a cavity mirror in the laser oscillator, another possible method is to introduce a known amount of glass into the beam path. Changing ϕ corresponds to delaying the envelope with respect to the carrier. This is equivalent to reducing the group velocity v_{group} with respect to the phase velocity v_{phase} of light, which can be achieved with normal dispersion of glass. At a central wavelength of 760 nm adding 52 μm of fused silica changes the phase by 2π without significantly affecting the pulse duration. A pair of glass wedges (apex angle 2.8°), one of which is driven by a stepper motor ($\Delta x = \Delta s \tan(2.8°)$ glass is introduced by a horizontal movement of Δs), is used here. The stabilization can thus be operated completely independently of the laser system as such.

Figure 4 also shows the idea of phase stabilization. If a positive error signal is recorded, a proportional amount of glass is introduced (i.e., the carrier-envelope phase is increased). Vice versa, if a negative error signal is recorded, a proportional amount of glass is removed (i.e., the carrier-envelope phase is decreased). With this procedure, there are two equilibrium positions, A and B, where the error signal is zero. Only position B is characterized by a stable equilibrium. The phase will therefore be stabilized to the corresponding value, in this case slightly higher than π. Stabilizing to different phase values is still possible by using a suitable offset for evaluating the error signal. Best results are expected however, where the slope of the error signal is largest, i.e., around zero. Furthermore, if one were to try to stabilize to a value coincident or close to an extremum of the error signal, the procedure would not converge. A more robust approach for stabilizing to an arbitrary value of the phase relies on simultaneous evaluation of error signals corresponding to different energy windows, because the relative positions of the respective extrema are different.

4 Results

In order to test the capability of the stereo-ATI apparatus for correcting low-frequency phase drifts, two basic experiments were performed. First, a slow, constant, and known carrier-envelope phase drift is applied by changing the amount of glass in the beam path by means of an additional pair of wedges. The stereo-ATI servo loop then drives the 'corrective' pair of wedges, as explained above. If the material and geometry of the two pairs of wedges are equal, their movement is expected to be identical but in opposite directions.

Figure 5a shows the corresponding measurement. The first pair of wedges (dotted line) was moved at different speeds in both directions. The amount of glass introduced can be directly translated to a phase value. The movement of the second pair of wedges (lower gray line), controlled by the ATI signal, compensates in real time the phase drift deliberately introduced by the first. The resulting phase (black line) is constant within an error not exceeding 0.5 rad, while the phase drift covered considerably more than 6 rad. Panel b of the same figure shows the measured left/right asymmetry over the full electron spectra. The overall features are preserved during the measurement. This proves the capability of the stereo-ATI experiment of fully correcting phase drifts of more than π rad / min. Thorough examination reveals a slight shift in the spectra when the applied phase drift is fast (between B and C). This is to be expected, since the temporal sequence of subsequent steps in this setup was (i) change the 'error' wedges, then (ii) measure the phase, and finally (iii) correct it by moving the 'corrective' wedges. It should also be borne in mind that typical phase drifts of the laser system without this additional servo loop are of the order of 50 mrad / min, more than two orders of magnitude less than in this example. Even here, as soon as the artificial phase drift stops, the initial spectral properties and thus the phase are quickly restored (see interval from C to D).

The second test aims at restoring the phase ϕ after it has been completely lost due to an external disturbance (e.g., laser readjustment). The stereo-ATI phase meter also offers a solution to this problem. Running the stabilization procedure in order to control the position of the 'corrective' glass wedge automatically stabilizes the phase exactly to the previous value. This is illustrated in Fig. 6, showing the carrier-envelope phase (deduced from the position of the 'corrective' pair of wedges) as a function of time. At the instants A, B, and C, the phase was intentionally changed by a large amount by externally changing the wedge position. This is analogous in all respects to relocking the phase to a different value after laser readjustment. Subsequently, the servo loop takes action

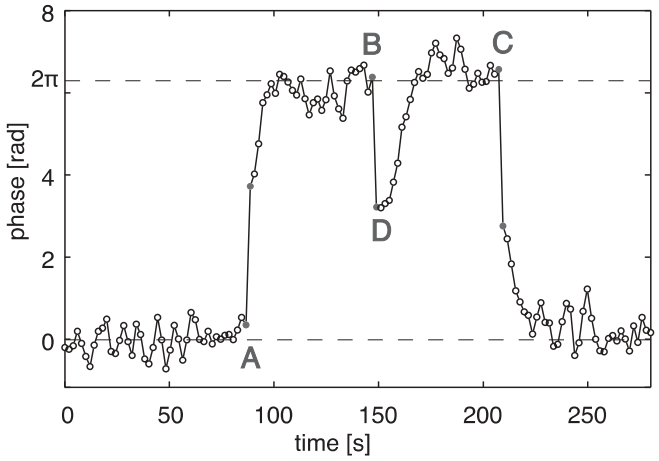

FIGURE 6 Position of the 'corrective' glass wedge (translated in phase value) as a function of time. At the instants A, B, and C, large phase jumps were applied, and the phase is subsequently automatically recovered within an acceptable error. Note that, depending on where the closest stable position is, the automatic procedure either increases (after transitions A and B) or decreases (after transition C) the glass thickness. Note also the short-term stability D just after transition B, originating from the unstable equilibrium position shifted by π with respect to the stable one (see Fig. 4)

and ϕ soon reaches its initial value (modulo 2π). In some cases the stabilization can be slowed down in a locally stable phase region (Fig. 6 D and Fig. 4 A), but an appropriate algorithm or the concurrent use of error signals from different energy windows Fig. 4 is able to avoid this.

The rather high noise in these two examples is due to pulse durations being not fully optimized. Accordingly, the contrast of the left/right signal was rather low. Longer integration times for each phase measurement can always minimize the noise.

5 Conclusion

A novel scheme to stabilize the carrier-envelope phase ϕ for an in principle unlimited time has been demonstrated. Even after a complete loss of stabilization the described stereo-ATI stabilization loop can restore the phase initially chosen. This was demonstrated in a recent experiment with a momentum spectrometer [11]. Such experiments have hitherto not been possible, since a measurement time of several hours for each carrier-envelope phase chosen was required.

Another appealing aspect of the ATI phase meter is the small amount of power ($< 20\,\mu$J) needed. Basically all the laser power is thus available for other experiments. Future technical improvements should further decrease the energy required, allowing also higher-repetition-rate lasers to operate simultaneous experiments. Another benefit is that the target gas pressure is so low ($p < 10^{-4}$ mbar) that the ATI experiment does not affect the laser beam. The stereo-ATI apparatus can thus be placed anywhere in a beam line. In principle, if a long focus were available, it would even be possible to place the stereo-ATI and a second experiment in a single vacuum chamber, allowing real-time calibration and stabilization of the carrier-envelope phase.

The current disadvantage is the small bandwidth of the stabilization scheme, which limits its suitability to correcting only long-term phase drifts. Modifications to the acquisition of the electron spectra are being investigated with the ultimate aim of completely replacing the currently used second f-to-$2f$ servo loop, with the setup described here.

ACKNOWLEDGEMENTS This work was supported by the German Research Foundation (Grant No. PA730/2), the Welch Foundation (Grant No. A-1562), and the Austrian Science Fund (Grants No. F016, No. Z63, and No. P15382).

REFERENCES

1 M. Nisoli, S. De Silvestri, O. Svelto: Appl. Phys. Lett. **68**, 2793 (1996)
2 M. Nisoli, S. De Silvestri, O. Svelto, R. Szipőcs, K. Ferencz, C. Spielmann, S. Sartania, F. Krausz: Opt. Lett. **22**, 522 (1997)
3 L. Xu, C. Spielmann, A. Poppe, T. Brabec, F. Krausz, T.W. Hänsch: Opt. Lett. **21**, 2008 (1996)
4 G.G. Paulus, F. Grasbon, H. Walther, P. Villoresi, M. Nisoli, S. Stagira, E. Priori, S. De Silvestri: Nature **414**, 182 (2001)
5 J. Reichert, R. Holzwarth, T. Udem, T.W. Hänsch: Opt. Commun. **172**, 59 (1999)
6 H.R. Telle, G. Steinmeyer, A.E. Dunlop, J. Stenger, D.H. Sutter, U. Keller: Appl. Phys. B **69**, 327 (1999)
7 D.J. Jones, S.A. Diddams, J.K. Ranka, A. Stentz, R.S. Windeler, J.L. Hall, S.T. Cundiff: Science **288**, 635 (2000)
8 A. Apolonski, A. Poppe, G. Tempea, C. Spielmann, T. Udem, R. Holzwarth, T.W. Hänsch, F. Krausz: Phys. Rev. Lett. **85**, 740 (2000)
9 A. Baltuška, T. Udem, M. Uiberacker, M. Hentschel, E. Goulielmakis, C. Gohle, R. Holzwarth, V.S. Yakovlev, A. Scrinzi, T.W. Hänsch, F. Krausz: Nature **421**, 611 (2003)
10 G.G. Paulus, F. Lindner, H. Walther, A. Baltuška, E. Goulielakis, M. Lezius, F. Krausz: Phys. Rev. Lett. **91**, 253 004 (2003)
11 X. Liu, H. Rottke, E. Eremina, W. Sandner, E. Goulielmakis, K.O. Keeffe, M. Lezius, F. Krausz, F. Lindner, M.G. Schätzel, G.G. Paulus, H. Walther: submitted to Phys. Rev. Lett.
12 A. de Bohan, P. Antoine, D.B. Milošević, B. Piraux: Phys. Rev. Lett. **81**, 1837 (1998)
13 G. Sansone, C. Vozzi, S. Stagira, M. Pascolini, L. Poletto, P. Villoresi, G. Tondello, S. De Silvestri, M. Nisoli: Phys. Rev. Lett. **92**, 113 904 (2004)
14 E. Cormier, P. Lambropoulos: Eur. Phys. J. D **2**, 15 (1998)
15 P. Dietrich, F. Krausz, and P.B. Corkum: Opt. Lett. **25**, 16 (2000)
16 D.B. Milošević, G.G. Paulus, W. Becker: Phys. Rev. Lett. **89**, 153 001 (2002)
17 S. Chelkowski, A.D. Bandrauk: Phys. Rev. A **65**, 061 802 (2002)
18 D.B. Milošević, G.G. Paulus, W. Becker: Opt. Ex. **11**, 1418 (2003)
19 X. Liu, F. de Morisson Faria: Phys. Rev. Lett. **92**, 133 006 (2004)
20 A. Poppe, R. Holzwarth, A. Apolonski, G. Tempea, C. Spielmann, T.W. Hänsch, F. Krausz: Appl. Phys. B **72**, 373 (2001)
21 T. Udem, J. Reichert, R. Holzwarth, T.W. Hänsch: Phys. Rev. Lett. **82**, 3568 (1999)
22 R. Szipőcs, K. Ferencz, C. Spielmann, F. Krausz: Opt. Lett. **19**, 201 (1994)
23 P. Dombi, A. Apolonski, C. Lemell, G.G. Paulus, M. Kakehata, R. Holzwarth, T. Udem, K. Torizuka, J. Burgdörfer, T.W. Hänsch, F. Krausz: New J. Phys. **6**, 39 (2004)
24 P. Agostini, F. Fabre, G. Mainfray, G. Petite, N.K. Rahman: Phys. Rev. Lett. **42**, 1127 (1979)
25 P.B. Corkum: Phys. Rev. Lett. **71**, 1994 (1993)
26 W. Becker, F. Grasbon, R. Kopold, D.B. Milošević, G.G. Paulus, H. Walther: Adv. At. Mol. Opt. Phys. **48**, 35 (2002) 35
27 G.G. Paulus, W. Nicklich, H. Xu, P. Lambropoulos, H. Walther: Phys. Rev. Lett. **72**, 2851 (1994)
28 A. Baltuška, M. Uiberacker, E. Goulielmakis, R. Kienberger, V.S. Yakovlev, T. Udem, T.W. Hänsch, F. Krausz: IEEE J. Sel. Top. Quant. Electron. **9**, 972 (2003)
29 F. Grasbon, G.G. Paulus, H. Walther, P. Villoresi, G. Sansone, S. Stagira, M. Nisoli, S. De Silvestri: Phys. Rev. Lett. **91**, 173 003 (2003)